

# INFLUENCE OF NOTCH ROOT RADIUS ON THE FRACTURE BEHAVIOR OF AISI 4140 STEEL AUSTENITIZED AT LOW AND HIGH TEMPERATURES

M. L. Graça, F. A. Darwish and L. C. Pereira\*

*Department of Materials, Science and Metallurgy, Catholic University (PUC/RJ) Rio de Janeiro, RJ, Brazil*  
*\*COSIPA, Santos, SP, Brazil*

## ABSTRACT

A study has been made of the influence of notch root radius on the ambient temperature toughness of commercial AISI 4140 steel austenitized at 870 and 1200°C and tested in the as-quenched and quenched and tempered at 200 and 350°C conditions. Charpy specimens containing V-notches of different root radii were loaded to failure in three point slow bending. Toughness values were calculated and the specimens were fractographically examined. The results obtained are seen to confirm the concept of characteristic distance for failure as well as its validity to appropriately explain differences encountered in plane strain fracture toughness. The results also show that low temperature austenitizing invariably gives rise to superior rounded notch toughness as compared to high temperature austenitizing treatment. This observation is found to be associated with shear lip formation along the notch root for conventionally austenitized specimens. Shear lip width is seen to increase with the notch radius and with the tensile ductility of the material.

## KEYWORDS

Notch root radius, austenitizing temperature, low temperature tempering, fracture toughness, effective root radius, prior austenite, fractography, shear lip.

## INTRODUCTION

High temperature austenitizing treatment at 1200°C has been found to improve the plane strain fracture toughness,  $K_{Ic}$ , of as-quenched and of quenched and low temperature tempered high strength low alloy steels compared to conventional 870°C austenitizing (Datta, 1981; Datta and Wood, 1981; Firrao and co-workers, 1982; Lai and co-workers, 1974; Ritchie, Francis and Server, 1976; Ritchie and Horn, 1978; Ritchie and Knott, 1974; Wood, 1975; Youngblood and Raghavan, 1977; Zackay and co-workers, 1972). On the other hand rounded notch tests have been shown to yield higher toughness values for conventionally heat treated specimens (Datta, 1981; Datta and Wood, 1981; Firrao and co-workers, 1982; Ritchie, Francis and Server, 1976; Ritchie and Horn, 1978),

thus indicating that high temperature austenitizing is detrimental to fracture resistance in the presence of blunt notches. The increase in  $K_{IC}$  with increasing austenitizing temperature was considered to be associated with an increase in the characteristic distance for fracture, whereas the decrease in rounded notch toughness,  $K_A$ , was interpreted in terms of a reduction in critical fracture stress,  $\sigma_f$ , or critical fracture strain,  $\epsilon_f$ , depending on the operating fracture mode (Ritchie, Francis and Server, 1976; Ritchie and Horn, 1978).

Experimentally the characteristic distance for failure is represented by the effective notch root radius,  $\rho_{eff}$ , below which the apparent toughness,  $K_A$ , remains constant and equal to  $K_{IC}$  (Ritchie, Francis and Server, 1976; Ritchie and Horn, 1978). However for a variety of testing conditions, the results obtained by Datta (1981) did not reveal the occurrence of an effective root radius in as-quenched and quenched and low temperature tempered AISI 4340 steel specimens. Hence he concludes that the explanation based on constant limiting root radius for the improvement in  $K_{IC}$  accompanying high temperature austenitizing does not seem to be valid. More recently Firrao and co-workers (1982) have verified the occurrence of an effective root radius in AISI 4340 specimens quenched from 870°C. For  $\rho > \rho_{eff}$ , the fracture surfaces are seen to be characterized by a continuous shear lip formation along the notch root, whereas in specimens with  $\rho < \rho_{eff}$  a stress controlled fracture mechanism is shown to be active. On the other hand, no shear lip formation has been recorded as  $\rho$  goes beyond  $\rho_{eff}$  in specimens step quenched from 1200°C and fracture morphology remained essentially the same (intergranular and quasicleavage).

It is the purpose of the present work to investigate the influence of austenitizing temperature on the relationship between fracture toughness and notch root radius for commercial AISI 4140 high strength steel in the as-quenched and quenched and tempered conditions. This relationship is utilized to determine the effective root radius which is then correlated with microstructural aspects of the material. The values obtained as well as overall fractographic features of fractured specimens are combined to explain the difference in toughness encountered for AISI 4140 steel tested in different microstructural conditions.

#### MATERIAL AND EXPERIMENTAL METHODS

The material used in this investigation was AISI 4140 hot rolled one inch thick plate, having the following composition (wt pct):

C	Mn	P	S	Si	Cr	Mo	Ni
0.38	0.78	0.014	0.024	0.29	0.90	0.17	0.25

Standard sized Charpy bars were machined out of the as-received plate parallel to the rolling direction. Deep V-notches were milled to depth-to-specimen width ratio,  $a/W$ , of 0.5, employing a series of constant profile cutters with different point radii and the resulting root radii were projected on a screen and measured at 20X.

The test specimens were heat treated by austenitizing for 30 minutes at temperatures of 870 and 1200°C in a neutral salt bath followed by quenching in agitated oil. The tempering treatment was carried out in a chamber furnace for 1 hour at temperatures of 200 and 350°C. Six distinct microstructures were thus obtained and are termed 870+Q, 870+200, 870+350, 1200+Q, 1200+200 and 1200+350, where Q indicates the material in the as-quenched condition. The

resulting tensile properties are given in Table 1. After heat treatment, the

TABLE 1 Tensile Properties for the Different Heat Treatments

Heat Treatment	Yield Stress*(MPa)	Ultimate Stress(MPa)	Elongation(%)
870+Q	1,333	1,902	4.2
870+200	1,351	1,794	10.1
870+350	1,327	1,559	9.6
1200+Q	1,127	1,819	3.8
1200+200	1,224	1,451	3.4
1200+350	1,140	1,255	2.4

\*represented by the 0.2% proof stress.

notch root radii were rechecked by projecting them on a viewing screen at 20X. Fatigue precracking was carried out after heat treatment on standard Charpy specimens ( $a/W = 0.2$ ) to final  $a/W$  of about 0.5.

The test specimens were fractured at room temperature in three point bending, using an Instron universal testing machine at a displacement rate ranging from 0.25 mm/min for fatigue precracked specimens to 7 mm/min for specimens with 1 mm notch root radius.

Only the specimens that failed before general yielding were considered and the J-integral values for fracture initiation,  $J_A$ , were thus calculated from the maximum load, modulus of elasticity E and the specimen compliance, using Rice estimation formula (Rice, Paris and Merkle, 1973; Server, 1978). The obtained  $J_A$  values, termed  $J_{IC}$  for fatigue precracked specimens, were found to satisfy the validity criterion related to specimen dimensions (Server, 1978) and were used to estimate  $K_A$  from the relation

$$K_A = \left( \frac{E J_A}{1-\nu^2} \right)^{1/2}, \quad (1)$$

where  $\nu$  is Poisson's ratio. Toughness calculation from linear elastic fracture mechanics equations resulted in slightly lower values (compared to those obtained from equation (1)) which, except for a few precracked specimens, did not satisfy the ASTM E399 size criterion.

#### RESULTS

Critical fracture stress and critical fracture strain models (Ritchie, Francis and Server, 1976; Ritchie and Horn, 1978) predict a linear relationship between the apparent toughness and  $\rho^{1/2}$ . Accordingly the  $K_A$  values obtained from slow bend tests are given in Fig. 1 as a function of  $\rho^{1/2}$ . One can notice that, for specimens tested in the as-quenched (untempered) and quenched and tempered at 200 and 350°C conditions, the 1200°C austenitizing treatment invariably results in larger effective root radius, in higher  $K_{IC}$  and in lower  $K_A$  as compared to conventional 870°C austenitizing. As  $\rho$  increases, fracture toughness data from specimens tested in the 870+Q and 870+350 conditions are seen to follow a second sloped line (Fig. 1). This might indicate a continuous decrease in notch tip strain with the increase in notch root radius (Firrao and co-workers, 1982).

Fractographic studies have indicated that failure occurs primarily by intergranular cracking in specimens obtained by tempering at 350°C and that in the

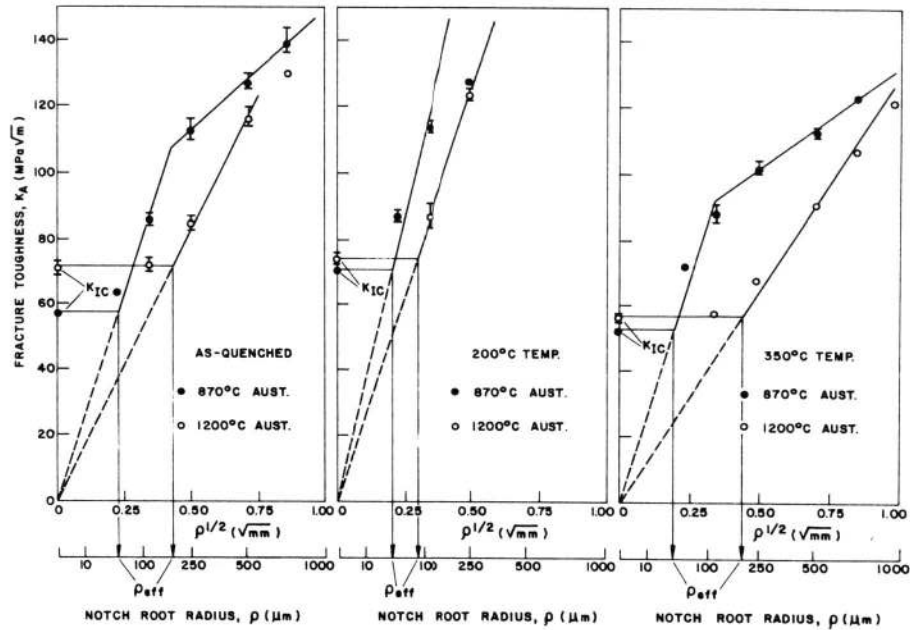


Fig. 1. Relationship between toughness and notch root radius (each data point represents an average of three tests).

1200+Q condition the specimens fail by intergranular and quasicleavage. However it is observed that specimens corresponding to the 870+350 heat treatment condition are characterized by a continuous shear lip formation along the notch root for  $\rho \geq 50 \mu\text{m}$  and that the shear lip width,  $s$ , increases with  $\rho$ . On the other hand, no continuous shear lip formation was observed for specimens tested in the 1200+Q and 1200+200 conditions.

Fractographic examination of the specimens tested in the 870+200 condition has revealed that fracture initiates predominantly by ductile rupture. In the as-quenched condition, the conventionally austenitized specimens failed mainly in a ductile manner, but the fracture surfaces were also seen to display areas of quasicleavage. Again the fracture surfaces for these two cases are seen to be characterized by the formation of shear lips at the notch root for  $\rho \geq 50 \mu\text{m}$ . In regard to specimens in the 1200+200 condition, their fracture surfaces have been found to display a mixture of ductile rupture, intergranular and quasicleavage. Continuous shear lip formation along the notch root was not observed.

Examples of fracture surfaces as observed by the scanning electron microscope (SEM) are shown in Fig. 2. The relationship between the shear lip width,  $s$ , and the notch root radius,  $\rho$ , is depicted in Fig. 3 for the cases where continuous shear lip formation was observed along the notch root.

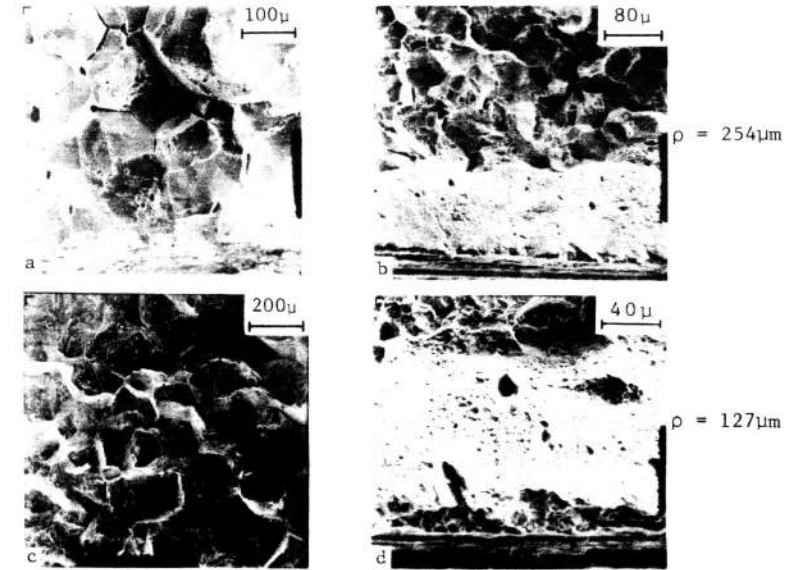


Fig. 2. SEM of fracture surfaces for, (a) 1200+350, (b) 870+350, (c) 1200+Q and (d) 870+200 conditions (note shear lip formation along notch root for (b) and (d)).

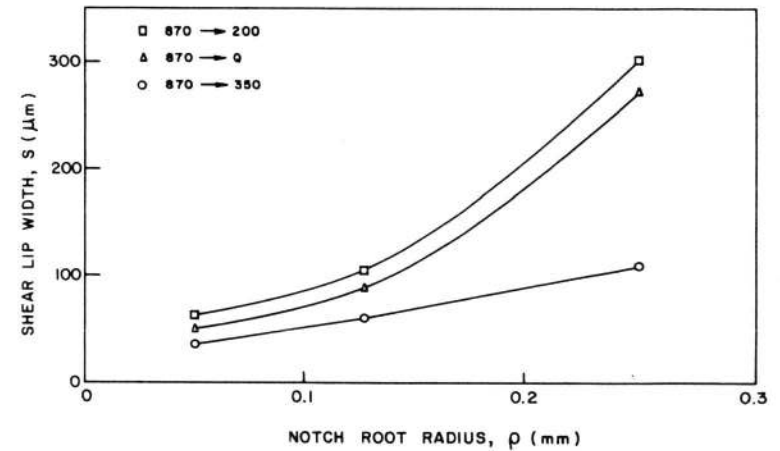


Fig. 3. Variation of shear lip width with notch root radius.

DISCUSSION

The slope of the straight lines passing through the origin in Fig. 1 is re-

lated to the critical fracture stress,  $\sigma_f$ , and to the critical fracture strain,  $\epsilon_f$ , in stress controlled and strain controlled failure, respectively. Using the yield limit values given in Table 1,  $\sigma_f$  and  $\epsilon_f$  were thus calculated from (Ritchie, Francis and Server, 1976; Ritchie and Horn, 1978)

$$K_A \approx 2.9 \sigma_y [\exp(\sigma_f/\sigma_y - 1)]^{1/2} \rho^{1/2} \quad \rho \geq \rho_{\text{eff}} \quad (2)$$

$$\text{and} \quad K_A \approx \left(\frac{3}{2} \sigma_y E \epsilon_f\right)^{1/2} \rho^{1/2} \quad \rho \geq \rho_{\text{eff}} \quad (3)$$

where  $\sigma_y$  is the yield limit. The resulting values are depicted in Table 2, together with  $\rho_{\text{eff}}$  and prior austenite grain size,  $d_a$ .

TABLE 2  $\rho_{\text{eff}}$ ,  $\sigma_f$ ,  $\epsilon_f$  and  $d_a$  for the Different Heat Treatments

Heat Treatment	$\rho_{\text{eff}}$ ( $\mu\text{m}$ )	$\sigma_f$ (MPa)	$\epsilon_f$ (%)	$d_a$ ( $\mu\text{m}$ )
870+Q	51	-	15.8	32
870+200	43	-	27.7	32
870+350	39	3,677	-	32
1200+Q	188	2,565	-	157
1200+200	91	-	-	157
1200+350	196	2,183	-	157

The room temperature fracture toughness results reported in Fig. 1 indicate that tempered martensite embrittlement (TME) has occurred in the steel after tempering at 350°C. However, based on the percentage loss in toughness, TME is seen to be more pronounced for the high temperature austenitizing. Now if one considers the fractographic features of the specimens tempered at 350°C, particularly the intergranular cleavage facet size (Fig. 2), one may conclude that the prior austenite grain boundaries were actually embrittled as a result of this treatment. This embrittling effect is believed to be related to a combination of impurity element segregation, notably P, and carbide formation at prior austenite grain boundaries (Banerji, McMahon and Feng, 1978; Briant and Banerji, 1979; Materkowski and Krauss, 1979; Ustinovshchikov, 1983). These grain boundary carbides can act as slip barriers and help initiate intergranular cracks at the already weakened boundaries. While P segregation to prior austenite grain boundaries occurs during austenitization (Banerji, McMahon and Feng, 1978; Briant and Banerji, 1979), cementite forms by precipitation from the tempered martensite and by thermal decomposition of retained austenite films at prior austenite grain boundaries during tempering (Banerji, McMahon and Feng, 1978; Briant and Banerji, 1979; Horn and Ritchie, 1978; Materkowski and Krauss, 1979). Subsequent deformation-induced transformation on loading of remaining intergranular austenite (Horn and Ritchie, 1978) further contributes embrittling carbides (cementite) on prior austenite grain boundaries. At this point it should be mentioned that no attempt was made in this work to determine retained austenite distribution as a function of austenitization temperature. However transmission electron microscopy studies by Sastry and Wood (1980) have revealed the presence of retained austenite grain boundaries (in addition to interlath films of retained austenite) in coarse-grained AISI 4340 steel austenitized at 1200°C. On the other hand very little retained austenite was found to be present along the prior austenite grain boundaries in fine-grained structures (austenitized at 870°C). It is thus concluded that, despite increased P segregation to prior austenite grain boundaries for low temperature austenitizing, apparently higher carbide concentration at those boundaries for the 1200°C austenitizing seems respon-

sible for the lower  $\sigma_f$  associated with the latter treatment.

The arguments presented above are considered to be consistent with the fracture behavior, in particular the  $\sigma_f$  level, of the specimens tested in the 1200+Q condition. Here failure occurs by a mixture of intergranular and quasicleavage apparently as a result of P segregation to prior austenite grain boundaries during austenitizing combined with cementite formation due to deformation-induced transformation on loading of interlath and intergranular retained austenite.

Shear lip formation at notch root occurs in specimens tested in the 870+350 condition for  $\rho \geq 50 \mu\text{m} > \rho_{\text{eff}}$  and higher  $K_A$  values observed for these specimens as compared to the 1200+Q and 1200+350 conditions can be attributed in part to the occurrence of shear lips. The absence of these shear lips for fatigue precracked specimens was not associated with a change in fracture morphology, which remained essentially identical to that of areas adjacent to shear lips in specimens with  $\rho > \rho_{\text{eff}}$ . The plastic zone size at fracture can be estimated from critical fracture stress model and a value of about  $3\rho$  is obtained for the specimens tested in the 870+350 condition. Fracture thus initiates at such a distance from the notch tip and the resulting crack propagates in the notch plane. As the crack gets closer to the notch surface it starts to propagate by shear rupture giving rise to shear lip formation or it could end up joining a shear lip already emanating from the notch surface. Consistent with the findings by Firrao and co-workers (1982), the shear lip width increases with the increase in  $\rho$  (Fig. 3), probably as a result of less plastic constraint imposed by the notch as it gets blunter.

Observation of Table 2 points to the fact that for stress controlled fracture AISI 4140 steel exhibits an effective root radius of the order of the prior austenite grain size. This indicates that high temperature austenitization results in an increase in the characteristic distance ahead of the crack tip over which the critical stress  $\sigma_f$  must be exceeded for fracture to occur through a coarsening of the microstructure (associated with increased prior austenite grain size) (Ritchie, Francis and Server, 1976; Ritchie and Horn, 1978). The reported  $\rho_{\text{eff}}$  values, together with those of  $\sigma_f$ , can thus be used to rationalize the  $K_{\text{IC}}$  data for the case of stress controlled failure.

Table 2 indicates that  $\epsilon_f$  is higher for the 870+200 condition as compared to the 870+Q treatment, consistent with an observed increase in uniaxial tensile ductility due to low temperature tempering. This improvement in  $\epsilon_f$  is believed to be associated with the transfer of carbon from the dislocations, during low temperature tempering, to form fine carbide precipitate (essentially  $\epsilon$ -carbide). It is interesting to note that the formation of this fine precipitate also hardens the steel, though the net effect of the transfer process is seen to be small (Table 1).

For ductile rupture (Fig. 4), the effective root radius is likely to be associated with second phase particle spacing and distribution (Ritchie and Horn, 1978). Hence the observation that  $\rho_{\text{eff}}$  is smaller for the 870+200 than for the 870+Q condition (Table 2) is probably related to carbide precipitation during low temperature tempering.  $\rho_{\text{eff}}$  obtained for the 1200+200 condition probably reflects an average between the limiting root radius for a stress controlled and that for a strain controlled failure since fracture initiation occurs by a mixture of ductile rupture, intergranular and quasicleavage.

Shear lip formation along the notch root was observed for specimens tested in the 870+Q and 870+200 conditions with  $\rho \geq 50 \mu\text{m}$ . However, for a given root radius a larger shear lip width,  $s$ , is encountered for the low temperature

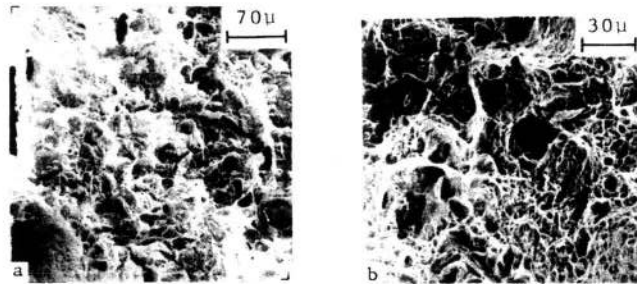


Fig. 4. Rupture dimples on the fracture surfaces for, (a) 870+Q and (b) 870+200 heat treatment conditions.

tempered material. This finding together with the difference in tensile ductility can explain why the blunt notch toughness should be higher for the 870+200 heat treated specimens as compared to the as-quenched (from 870°C) material. It is interesting to note that shear lip width is a reflection of the material's ductility. This is clearly demonstrated in Fig. 3 where one can notice that  $s$  is larger the higher the tensile ductility of the steel.

For fatigue precracked specimens no shear lip formation was observed and the fracture toughness ( $K_{IC}$  in this case) continued to be superior for the low temperature tempered conventionally austenitized specimens as compared to the ones in the as-quenched state. The observed difference in  $K_{IC}$  can be explained in terms of the reported values of  $\epsilon_f$  and  $\rho_{eff}$ .

In regard to the details of the initiation process in strain controlled fracture in blunt notch testing, it is not clear yet whether the critical event involves initiation at the notch tip in virtue of high local strain there or at some point removed from the tip due to increased triaxiality.

#### CONCLUSIONS

The characteristic distance concept seems to be appropriate for explaining differences in plane strain fracture toughness encountered in the course of testing low and high temperature austenitized AISI 4140 steel in the as-quenched and quenched and tempered conditions.

The superior apparent toughness values observed for conventional 870°C austenitizing as compared to high temperature austenitizing seem to be associated with the formation of shear lips along the notch root. Shear lip width is seen to increase with the increase in tensile ductility of the conventionally austenitized material.

No significant change in fracture features is detected as  $\rho$  is decreased below the effective root radius. However for the conventionally austenitized material the shear lips are seen to disappear as verified for the fatigue precracked specimens.

For stress controlled failure the critical fracture stress  $\sigma_f$  seems to be the main factor in defining the apparent toughness  $K_A$ , whereas in strain control-

led failure  $\epsilon_f$  assumes this role.

#### ACKNOWLEDGEMENT

The authors wish to thank Mr. C.R. Ouro and Mr. J.C. Teixeira for valuable discussions. Financial support by FINEP, CNPq, and CNEN is gratefully acknowledged. Thanks are also due to CSN for supplying the material used in this work and to IME/RJ for using the scanning electron microscope.

#### REFERENCES

- Banerji, S.K., McMahon, C.J., Jr. and Feng, H.C. (1978). *Metall. Trans.* **9A**, 237-247.
- Briant, C.L. and Banerji, S.K. (1979). *Metall. Trans.* **10A**, 1729-1737.
- Datta, K.P. (1981). *Mater. Sci. Eng.* **51**, 241-252.
- Datta, K.P. and Wood, W.E. (1981). *J. Testing and Evaluation* **9**, 111-117.
- Firrao, D., Begley, J.A., Silva, G., Roberti, R. and de Benedetti, B. (1982). *Metall. Trans.* **13A**, 1003-1013.
- Horn, R.M. and Ritchie, R.O. (1978). *Metall. Trans.* **9A**, 1039-1053.
- Lai, G.Y., Wood, W.E., Clark, R.A., Zackay, V.F. and Parker, E.R. (1974). *Metall. Trans.* **5**, 1663-1670.
- Materkowski, J.P. and Krauss, G. (1979). *Metall. Trans.* **10A**, 1643-1651.
- Rice, J.R., Paris, P.C. and Merkle, J.G. (1973). *ASTM STP 536*, American society, for Testing and Materials, 231-245.
- Ritchie, R.O., Francis, B. and Server, W.L. (1976). *Metall. Trans.* **7A**, 831-838.
- Ritchie, R.O. and Horn, R.M. (1978). *Metall. Trans.* **9A**, 331-341.
- Ritchie, R.O. and Knott, J.F. (1974). *Metall. Trans.* **5**, 782-785.
- Sastry, C.N. and Wood, W.E. (1980). *Mater. Sci. Eng.* **45**, 277-280.
- Server, W.L. (1978). *J. Testing and Evaluation* **6**, 29-34.
- Ustinovshchikov, J.I. (1983). *Acta Metall.* **31**, 355-364.
- Wood, W.E. (1975). *Eng. Fract. Mech.* **7**, 219-234.
- Youngblood, J.L. and Raghavan, M. (1977). *Metall. Trans.* **8A**, 1439-1448.
- Zackay, V.F., Parker, E.R., Goolsby, R.D. and Wood, W.E. (1972). *Nature Phys. Sci.* **236**, 108-109.